The Journal of Nutrition
Nutrition and Disease

Adverse Maternal Environment and Postweaning Western Diet Alter Hepatic CD36 Expression and Methylation Concurrently with Nonalcoholic Fatty Liver Disease in Mouse Offspring

Qi Fu,[1] Paula E North,[2] Xingrao Ke,[1] Yi-Wen Huang,[3] Katie A Fritz,[4] Amber V Majnik,[4] and Robert H Lane[5]

[1]Department of Research Administration, Children's Mercy Hospital, Kansas City, MO, USA; [2]Department of Pediatric Pathology, Medical College of Wisconsin, Milwaukee, WI, USA; [3]Department of Obstetrics & Gynecology, Medical College of Wisconsin, Milwaukee, WI, USA; [4]Department of Pediatrics, Medical College of Wisconsin, Milwaukee, WI, USA; and [5]Department of Administration, Children's Mercy Hospital, Kansas City, MO, USA

ABSTRACT

Background: The role of an adverse maternal environment (AME) in conjunction with a postweaning Western diet (WD) in the development of nonalcoholic fatty liver disease (NAFLD) in adult offspring has not been explored. Likewise, the molecular mechanisms associated with AME-induced NAFLD have not been studied. The fatty acid translocase or cluster of differentiation 36 (CD36) has been implicated to play a causal role in the pathogenesis of WD-induced steatosis. However, it is unknown if CD36 plays a role in AME-induced NAFLD.

Objective: This study was designed to evaluate the isolated and additive impact of AME and postweaning WD on the expression and DNA methylation of hepatic *Cd36* in association with the development of NAFLD in a novel mouse model.

Methods: AME constituted maternal WD and maternal stress, whereas the control (Con) group had neither. Female C57BL/6J mice were fed a WD [40% fat energy, 29.1% sucrose energy, and 0.15% cholesterol (wt/wt)] 5 wk prior to pregnancy and throughout lactation. Non invasive variable stressors (random frequent cage changing, limited bedding, novel object, etc.) were applied to WD dams during the last third of pregnancy to produce an AME. Con dams consumed the control diet (CD) (10% fat energy, no sucrose or cholesterol) and were not exposed to stress. Male offspring were weaned onto either CD or WD, creating 4 experimental groups: Con-CD, Con-WD, AME-CD, and AME-WD, and evaluated for metabolic and molecular parameters at 120 d of age.

Results: AME and postweaning WD independently and additively increased the development of hepatic steatosis in adult male offspring. AME and WD independently and additively upregulated hepatic CD36 protein and mRNA expression and hypomethylated promoters 2 and 3 of the *Cd36* gene.

Conclusions: Using a mouse AME model together with postweaning WD, this study demonstrates a role for CD36 in AME-induced NAFLD in offspring and reveals 2 regions of environmentally induced epigenetic heterogeneity within *Cd36*. *J Nutr* 2021;151:3102–3112.

Keywords: NAFLD, CD36, perinatal, methylation, DNA, maternal environment

Introduction

The incidence of NAFLD is steadily increasing and occurs in ~30% of Americans (1–3). Consumption of a high-fat diet (HFD) or Western diet (WD) contributes to the development of NAFLD. Interestingly, the incidence of adult NAFLD also increases following exposure to an adverse maternal environment (AME) (4–9). It is unclear if the development of NAFLD following an AME occurs via a similar mechanism to diet- related NAFLD.

The development of NAFLD following the consumption of HFD or WD occurs in part through the hepatic uptake of fatty acids in excess of metabolic requirements. Excess fatty acids are then stored inside hepatocytes and result in steatosis (10). Increasing numbers of studies have shown the role of the fatty acid translocase or cluster of differentiation 36 (CD36) in

© The Author(s) 2021. Published by Oxford University Press on behalf of the American Society for Nutrition. This is an Open Access article distributed under the terms of the Creative Commons Attribution-NonCommercial License (http://creativecommons.org/licenses/by-nc/4.0/), which permits non-commercial re-use, distribution, and reproduction in any medium, provided the original work is properly cited. For commercial re-use, please contact journals.permissions@oup.com
Manuscript received March 31, 2021. Initial review completed April 21, 2021. Revision accepted July 1, 2021.
First published online September 6, 2021; doi: https://doi.org/10.1093/jn/nxab249.

driving the onset of hepatic steatosis (4, 11, 12). CD36 plays a key role in increasing fatty acid uptake in hepatocytes and other cell types in the liver (10, 13, 14).

CD36 is a member of the class B scavenger receptor family and mediates long-chain fatty acid uptake in many tissues (15). CD36 also regulates lipid homeostasis in many cell types through multiple mechanisms, including regulation of fatty acid oxidation (16), VLDL secretion (17), and lipophagy (18). CD36 expression is low in hepatocytes but increases with lipid-rich diets and in NAFLD in both human and mouse models (19–23). A liver-specific *Cd36* knockout attenuates steatosis in mouse models of NAFLD (4, 12). Overexpression of hepatic CD36 resulted in a marked increase in hepatic fatty acid uptake and storage in both primary cultured hepatocytes and mouse livers (11). These indicate that CD36 expression has significant effects on liver lipid content and plays a causal role in the pathogenesis of NAFLD.

Multiple groups have studied the impact of maternal HFD or WD on the development of NAFLD in offspring in animal models (24–30). The offspring from these models developed NAFLD when fed a postweaning HFD or WD (5–9, 31). Despite this appreciation for the maternal and dietary impact on NAFLD, none of these studies ascertained if CD36 plays a role in AME-induced NAFLD.

To identify a mechanism through which relevant environmental stimuli alter CD36 expression, we have generated a novel AME model by combining long-term maternal WD and maternal stress. This combination of diet and stress was thoughtfully developed to model 2 of the most common environmental pressures during pregnancy as well as important factors for the development of NAFLD. Importantly, these factors are also modifiable and translatable from animals to humans.

Epigenetics, such as DNA methylation, provide insights into the mechanisms of early life predisposition to adult disease risk (32, 33). Understanding these epigenetic changes is important not only to understanding the mechanisms at play, but may also provide a molecular marker of potential disease. We hypothesized that, like HFD, AME induction of NAFLD will increase CD36 expression and that the addition of a postweaning WD will further increase CD36 expression and NAFLD. Additionally, AME-driven increase in CD36 will be accompanied by decreased methylation at key regulatory regions of *Cd36*.

Methods

Animals

All animal procedures were approved by the Medical College of Wisconsin Institutional Animal Care and Use Committee. This mouse model of AME has been previously published by our group (34). Briefly, Female C57BL/6J mice were maintained with standard light cycles at a constant temperature of 23°C with food and water available ad libitum. The mice were randomly allocated to either an experimental WD or a control diet (CD) (**Table 1** and **Supplemental Table 1**). The WD (D12079B, Research Diets, New Brunswick, NJ) has been previously published by other groups (35). It contained increased fat (40% compared with 10% in kcal), sucrose (29.1% compared with 0% in kcal), and cholesterol [0.15% compared with 0% (wt/wt)] compared with the CD (D14020502, Research Diets). The diets were provided for 5 wk before the females were mated with males receiving Laboratory Rodent Diet (5L0D, LabDiet), throughout pregnancy, and during lactation.

Dams fed the WD experienced a "stressed" environment during the last third of pregnancy. The combination of chronic WD and gestational stress is designated as AME (34). Briefly, the stressed environment consisted of daily random environmental changes as well as a static change in the maternal environment consisting of one-third of the standard amount of bedding from embryonic day (E)13 to E19. The daily random environmental changes included altered light cycles on 3 nonconsecutive d, 3 repeat cage changes throughout the day on E15, and the short-term introduction of a novel object in the cage for a day. Control (Con) dams consumed CD and were not exposed to stress (34). Food intake in dams was recorded from E6 through E19. At the end of pregnancy, 6 pregnant female mice from both Con and AME groups were anesthetized with isoflurane and killed by decapitation after 5 h of fasting. Trunk blood and serum were collected for the measurement of corticosterone. On postnatal day 5, litters were randomly culled to 6, 3 of each sex. Male offspring from both the Con and AME dams were weaned onto either the CD or WD, generating 4 experimental groups: Con-CD, Con-WD, AME-CD, and AME-WD (34). At the age of 120 d ($n = 6$ litters of each of the 4 groups, respectively) mice were anesthetized with isoflurane and killed by decapitation after 5 h of fasting. Trunk blood and serum were collected. Fasting glucose was measured using a OneTouch Verio IQ meter (LifeScan Inc.). Retroperitoneal fat pads and livers were quickly removed, and the wet weights were recorded. A piece of the right medial lobe of the liver was fixed in 10% formalin, the remaining liver was flash frozen in liquid nitrogen and stored in −80°C.

Serum concentrations of corticosterone, insulin, and alanine transaminase

Dam serum concentrations of corticosterone were measured by using a corticosterone enzyme immunoassay kit (Cat# K014-H1, Arbor assays) per the manufacturer's instructions.

Serum insulin was measured via the ELISA method using a Rat/Mouse Insulin ELISA kit (EMD Millipore) according to manufacturer's recommendations. HOMA-IR is widely used clinically for the diagnosis of human insulin resistance (IR). It has been validated in rats (36–38). It has been used as a diagnostic criterion for IR in mice studies, although it has not been validated in mice (39–42). HOMA-IR was calculated by using fasting insulin and fasting glucose In the following equation: HOMA-IR = fasting plasma insulin (in milliunits per liter) × fasting glucose (in millimoles per litter)/22.5 (43).

Serum ALT was measured by using EnzyChrom Alan Transaminase Assay Kit (BioAssay Systems) per the manufacturer's recommendations.

Glucose tolerance test (GTT)

The glucose tolerance test (GTT) was performed at week 14 of life after 6 h of fasting. Fasting glucose (time 0) was measured followed by intraperitoneal injection of glucose 60 mg in 20% (wt/vol) solution. The fixed dose of glucose was calculated as 2 g/kg of mean body weight of the Con-CD mice, based on the recommendations of the NIH Mouse Metabolic Phenotyping Center Consortium (44, 45). Glucose concentrations at 15, 30, 60, 90, and 120 min after glucose injection were measured using a OneTouch Verio IQ meter. Serum insulin was measured using ELISA at 60 min after glucose injection, as aforementioned.

The Department of Pediatrics, Medical College of Wisconsin supported the design, implementation, analysis, and interpretation of the data.
Author disclosures: The authors report no conflicts of interest.
Supplemental Tables 1–4 and Supplemental Figures 1–2 are available from the "Supplementary data" link in the online posting of the article and from the same link in the online table of contents at https://academic.oup.com/jn/.
Address correspondence to AVM (e-mail: amajnik@mcw.edu) and RHL (e-mail: rhlane@cmh.edu).
Abbreviations used: AME, adverse maternal environment; CD, control diet; CD36, fatty acid translocase or cluster of differentiation 36; Con, control; DHS, DNase I hypersensitive site; *Gadph*, glyceraldehyde-3-phosphate dehydrogenase; GTT, glucose tolerance test; HFD, high fat diet; *Hprt*, hypoxanthine guanine phosphoribosyl transferase; IHC, immunohistochemistry; IR, insulin resistance; NAFLD, nonalcoholic fatty liver disease; NAS, NAFLD activity score; NASH, nonalcoholic steatohepatitis; TSS, transcription start site; WD, Western diet.

TABLE 1 Compositions of experimental diets

	Diet			
	CD		WD	
Ingredients	g	kcal	g	kcal
Casein	195	780	195	780
DL-methionine	3	12	3	12
Corn starch	695	2780	50	200
Maltodextrin 10	150	600	100	400
Sucrose	0	0	341	1364
Milk fat, anhydrous	35.5	320	200	1800
Corn oil	17	153	10	90
Cellulose, BW200	50	0	50	0
Mineral mix S10001	35	0	35	0
Calcium carbonate	4	0	4	0
Vitamin mix V10001	10	40	10	40
Choline bitartrate	2	0	2	0
Cholesterol	0	0	1.5	0
Total	1196.6	4685	1001.5	4686
Protein, %	17	17	20	17
Carbohydrate, %	71	73	50	43
Fat, %	4	10	21	40
kcal/g	3.9		4.7	

CD, control diet (D14020502, Research Diets); WD, Western diet (D12079B, Research Diets).

Hepatic histology

Livers were fixed in 10% formalin and paraffin embedded.

Slices (4 μm) were stained by hematoxylin and eosin and Masson's trichrome. The NAFLD activity score (NAS) was proposed by the NIDDK-sponsored NASH Clinical Research Network and has been widely used for clinical trials in patients since its validation (46). NAS was evaluated by a pathologist blinded to the experimental groups by using the Kleiner scoring system (46). The score is defined as the unweighted sum of the scores for steatosis (0–3), lobular inflammation (0–3), and ballooning (0–2). A minimum of 5% steatosis (steatosis score of 1) was used for the operational minimal definition of histological NAFLD. NAS scores of 1–2 were largely considered mild NAFLD and 3–4 as moderate NAFLD. An NAS score of <2 was diagnosed as "not nonalcoholic steatohepatitis (NASH)." A score of ≥5 is interpreted as NASH.

RNA isolation

Total RNA isolation was performed by using an miRNeasy Mini Kit (Qiagen) following the manufacturer's instructions, including DNase I treatment. RNA was quantified spectrophotometrically. The integrity of RNA was assessed with an Agilent 2100 bioanalyzer in conjunction with the RNA 6000 Nano Kit (Agilent).

RT-PCR

cDNA was synthesized using a High-Capacity cDNA Reverse Transcription Kit (Applied Biosystems, Thermo Fisher Scientific). Real-time RT-PCR was performed as described earlier (47). Target primers and probes were either custom designed using the online PrimerQuest Tool [Integrated DNA Technologies (IDT)], or predesigned probe-based assays from IDT or Applied Biosystems, ThermoFisher Scientific (**Supplemental Table 2**). Real-time RT-PCR was performed on a ViiA 7 Real-Time PCR System (Applied Biosystems) in conjunction with a PrimeTime Gene Expression Master Mix (IDT). PCR conditions were 95°C for 10 min, followed by 40 cycles of 95°C for 15 s, and 60°C for 1 min. Samples were run in triplicate. Real-time RT-PCR quantitation was performed using hypoxanthine guanine phosphoribosyl transferase (*Hprt*) as an internal control. Based on the expression stability between experimental groups, *Hprt* was chosen as the internal control after assessing both *Hprt* and glyceraldehyde-3-phosphate dehydrogenase (*Gapdh*) as candidate housekeeping genes. Relative quantification of PCR products was based on value differences between the target and *Hprt* control using the comparative Ct method.

Cd36 mRNA variants were also quantified in the methods shown above using custom designed or predesigned primers/probes (Supplemental Table 2 and **Supplemental Figure 1**). Agarose electrophoresis of the PCR products of transcripts initiated from promoter 1 (P1 transcripts) revealed 2 bands, as did P2 transcripts. Each band was gel purified using a QIAquick Gel Extraction Kit (Qiagen). Sequences were confirmed by Sanger sequencing (Retrogen, Inc.). No specific assays can be designed for P3 transcripts because both P1 and P2 transcripts have 1 variant that crosses the exon 3–4 junction. We therefore calculated the relative amount of P3 transcripts by subtracting $2^{[-\Delta Ct\ (P1\ transcripts\ -\ Hprt)]}$ and $2^{[-\Delta Ct\ (P2\ transcripts\ -\ Hprt)]}$ from the $2^{[-\Delta Ct\ (total\ CD36\ -\ Hprt)]}$.

Membrane protein extraction and immunoblotting

Liver membrane protein was extracted using a Mem-PER Plus Membrane Protein Extraction Kit (Thermo Scientific) and quantified using a Pierce BCA Protein Assay Kit (Thermo Scientific).

Quantification of CD36 membrane protein was done using capillary immunoassay. Protein was separated and detected using a Wes Separation Capillary Cartridge 12–230 kDa along with a Wes Anti-Rabbit Detection Module (Simple Western system and Compass Software, Proteinsimple). Membrane protein samples were loaded at a 0.2-mg/mL dilution and rabbit antibody was used against CD36 (1:500) (ab133625, abcam) and pan Cadherin (1:5,000) (ab51034, abcam). Chemiluminescent signals shown as the peak area for anti-CD36 relative to that for anti-pan Cadherin were used as the levels of membrane CD36 protein relative to that of pan Cadherin.

Immunohistochemistry

Immunohistochemistry (IHC) analysis and staining were performed on formalin-fixed paraffin-embedded (FFPE) sections of mouse livers using the Bond RX autostainer platform (Leica Biosystems Inc.) in the Children's Research Institute Histology Core in Medical College of Wisconsin. Deparaffined sections underwent heat-induced epitope retrieval (Cat. No. S1699, pH 6.0, Agilent Dako) at 100°C for 20 min. The primary antibody was anti-CD36 rabbit monoclonal antibody (Cat. No. ab133625, abcam) at 1:100 dilution. Bound antibody was detected with biotinylated donkey anti-rabbit IgG (711-066-152, Jackson ImmunoResearch Laboratories, Inc.), streptavidin-HRP (P039701-2, Agilent Dako), and a DAB kit (K346811-2, Agilent Dako).

A negative control was prepared for all tissue samples by omitting the primary antibody. Macrophages, which strongly express CD36, provided an internal positive control (48).

Bisulfite pyrosequencing

Liver tissue was ground in liquid nitrogen and used for genomic DNA isolation with the DNeasy Blood & Tissue Kit (Qiagen) including RNase treatment. DNA quantity and purity were estimated spectrophotometrically. Briefly, spectrophotometry was done on a Biotek Cytation Hybrid Multi-Mode Reader with the Take 3 microvolume plate (Biotek) following the manufacturer's instructions. The ratio of the absorbance at 260 and 280 nm ($A_{260/280}$) >1.8 is considered "good purity."

Bisulfite treatment of genomic DNA was performed using an EpiTect Bisulfite Kit (Qiagen) as instructed in the manual. For each PCR, bisulfite-treated DNA equivalent to 20 ng of the DNA prior to bisulfite treatment was used.

Primers for PCR and sequencing were designed by using PyroMark Assay Design 2.0 software (Qiagen). Four amplicons around the 3 promoters were studied (**Supplemental Table 3**). The amplicons of Promoters 2 and 3 are in regulatory regions indicated by chromatin features of enhancer, promoter, promoter flank, and DNase I hypersensitive site (DHS) provided by Ensembl Regulatory Build (Ensembl.org) (49). Two CpG sites immediately upstream of the transcription start site (TSS) were chosen to be studied because the promoter 1 region does not have obvious DHS regions based on Ensembl.org. Three primer sets were also designed around regions in the intron 1 around −31 kb, −27.3 kb, and −13.4 kb upstream of exon 2 TSS because of the presence of regulatory chromatin features based on Ensembl.org (Supplemental Table 3). PCR conditions were 95°C for 10 min, followed by 50 cycles of 94°C for 30 s, primer-specific annealing temperature for 30 s, and 72°C for 30 s.

To avoid PCR artifacts which generate bias on the methylation status of CpG sites (50), annealing temperature was optimized using mouse methylated genomic DNA standards (EpigenDx, Inc.) as the DNA template. An annealing temperature that generated the percentage of CpG methylation closest to the known percentage of methylation in the methylation standard DNA was used for final experiments. Pyrosequencing was performed using Q48 Auroprep (Qiagen) in conjunction with PyroMark Q48 Advanced CpG Reagents (Qiagen) and PyroMark Q48 Magnetic Beads (Qiagen). Results were analyzed using Pyromark Q48 Autoprep software (Qiagen).

Laser capture microdissection followed by bisulfite pyrosequencing

Laser capture microdissection was performed using a PALM MicroBeam system (Zeiss Microscopy) with PALM Robo 3.2 software on a 10μm thickness of anti-CD36 IHC sections from the Con-CD group. Both CD36-positive ($CD36^+$) and -negative ($CD36^-$) hepatocytes were dissected. An EpiTect Fast FFPE Bisulfite Kit (Qiagen) was used for deparaffination, proteinase digestion, reverse crosslinking, and bisulfite conversion as instructed by the manufacturer's manual. PCR and pyrosequencing were performed as aforementioned.

Statistics

All analyses were performed using GraphPad Prism 8 software (GraphPad Software). The diagnosis of no, mild, or moderate NAFLD (based on the NAS score as described in the histology Method section) was analyzed using the χ^2 test. To determine the additive effect of AME and postweaning WD on the development of steatosis, a subtable with 2 categorical variables—the degree of insults [single insult (Con-CD and AME-WD combined) compared with double insults (AME-WD)] and the severity of steatosis—was created (51). Other data were analyzed for normality or lognormality first by using a Shapiro-Wilk normality test and Kolmogorov-Smirnov normality test with Dallal-Wilkinson-Lillie for the *P* value. All data except the serum ALT and food intake were normally distributed. Serum ALT was therefore analyzed by using a Kruskal-Wallis test followed by Dunn's multiple comparisons test to adjust the *P* value. Food mass and calorie intakes were analyzed using a Mann-Whitney test. The DNA methylation in the $CD36^+$ and $CD36^-$ hepatocytes was analyzed by using unpaired multiple t tests, followed by false discovery rate (FDR) testing by using the 2-stage step-up method of Benjamini et al. with desired FDR q <0.05 (52). All other data from the 4 groups were analyzed by using 2-way ANOVA to assess main and interaction effects, with diet and maternal environment as independent variables. When a significant main or interaction effect was detected, Bonferroni post hoc testing was used to identify the means that differ. When *P*-interaction was significant, a synergistic effect was reported. When significant *P* values of both AME-WD compared with AME-CD and AME-WD compared with Con-WD were found, but *P*-interaction was not significant, an additive effect was reported (51, 53). All data except the NAFLD diagnosis data were means ± SDs. The level of significance was set at $P < 0.05$ for all statistical tests.

Results

AME dams had elevated serum corticosterone concentrations

AME dams had significantly higher serum concentrations of corticosterone compared with Con dams at the end of pregnancy (**Table 2**). Serum corticosterone concentrations did not differ between the AME and Con offspring at birth, at weaning (data not shown), or at day 120 (34).

Consistently, the dams' food intake also indicated the impact of stress on AME dams. Stress significantly decreased food mass intake in the AME dams compared with Con dams during E13–E19 when stress was implemented (Table 2).

AME-WD significantly elevated liver weight in offspring

As our group has recently reported, all mice weaned onto the WD were significantly heavier than those weaned onto the CD, regardless of the maternal environments. This body weight difference was consistent with the significantly greater energy intake in the 2 WD groups compared with the 2 CD groups (34). The intake of diet mass was not different between the 4 groups (data not shown).

At day 120, both AME and postweaning WD significantly increased the ratio of retroperitoneal fat weight to body weight ($P < 0.0001$ and $P = 0.0009$; *P*-interaction ≥ 0.05) (**Table 3**). More importantly, postweaning WD augmented the AME effect on the increase of the ratio of liver to body weight (*P*-interaction = 0.0048) (Table 3).

AME-WD offspring developed IR

Neither postweaning WD nor AME affected fasting glucose (Table 3). However, WD and AME synergistically elevated both fasting insulin and HOMA-IR (*P*-interaction < 0.0001 and = 0.0013, respectively) (Table 3), indicating that postweaning WD exacerbated the predisposition of AME upon the development of IR in offspring.

These results were further supported by GTT. Only WD had a significant effect on the increase of blood glucose AUC during the GTT ($P = 0.0005$) (Table 3). In contrast, both WD and AME had significant effects on the increase of insulin concentrations 60 min after glucose injection ($P = 0.0025$ and 0.0011, respectively) (Table 3). A trend of significant interaction between WD and AME was observed for both the glucose AUC (*P*-interaction = 0.0676) and 60-min insulin concentrations (*P*-interaction = 0.051), indicating that AME induced in the offspring a greater predisposition to slower glucose clearance.

TABLE 2 Serum corticosterone concentrations and food intake in Con and AME dams

Dam group	Con	AME	*P* value
Serum corticosterone, ng/ml	32.7 ± 19.4	80.4 ± 50.6	0.0462
Food intake, g/d			
E6–E12	4.08 ± 0.452	4.93 ± 1.51	0.315
E13–E19	4.76 ± 0.539	3.71 ± 0.440	0.0009
Energy intake, kcal/d			
E6–E12	15.9 ± 1.76	23.2 ± 7.10	0.0003
E13–E19	18.6 ± 2.10	17.4 ± 2.07	0.397

Data are means ± SDs. $n = 8$. AME, adverse maternal environment; Con, maternal control group; E, embryonic day.

Taken together, these data indicate that AME-WD offspring developed IR at day 120 of age.

AME-WD offspring developed hepatic steatosis

In male offspring, postweaning WD alone (Con-WD) and AME alone (AME-CD) developed similar levels of mild steatosis (**Figure 1**A and B). These interesting results suggest that an adverse maternal environment has a long-term effect of steatosis, which is similar to the effect of an adult WD (Con-WD). More importantly, AME and postweaning WD had an additive effect on the development of steatosis, e.g., the AME-WD group had moderate but significantly more severe steatosis than the 2 single-insult groups combined (AME-CD and Con-WD) ($P < 0.0001$) (Figure 1A and B). There was no fibrosis in any specimens, confirmed by Trichrome staining (result not shown). Out of all the liver sections of the 4 groups evaluated, only 1 liver in the AME-WD group had lobular inflammation of the lowest level, which contributed to an NAS score of 1 to the sample. Additionally, AME-WD had elevated serum ALT concentrations compared with the corresponding control group (AME-CD) ($P = 0.0021$) (Figure 1C). This result indicates that postweaning WD exacerbated the effect of the maternal insults on hepatic steatosis.

AME and WD additively elevated hepatic *Cd36* mRNA expression

Among the genes important for fatty acid transport, oxidation, and synthesis, *Cd36* mRNA expression showed a distinctive expression pattern between the 4 experimental groups (**Figure 2** and **Supplemental Table 4**). Both WD and AME had significant effects on the increase of *Cd36* mRNA expression ($P = 0.0005$ and 0.0002, respectively). They additively further increased *Cd36* mRNA expression compared with WD alone ($P = 0.0022$) and the AME alone group ($P = 0.0043$) (*P*-interaction = 0.122) (Figure 2A and Supplemental Table 4).

We have also quantified the mRNA for genes related to hepatic inflammation, including *Mcp*1, *Il*1b, and *Tgfb*1. None of them revealed significant differences between groups (Supplemental Table 4), which is consistent with the histological findings.

AME and WD additively elevated hepatic CD36 protein expression

Mirroring the pattern of hepatic *Cd36* mRNA expression, postweaning WD and AME additively increased hepatic CD36 protein expression (*P*-interaction = 0.1731) (**Figure 3**A).

IHC staining for CD36 revealed a distinct lobular distribution pattern of $CD36^+$ hepatocytes in sections from the Con-CD, Con-WD, and AME-CD groups. The $CD36^+$ hepatocytes were found to be in locations surrounding the central veins, whereas periportal hepatocytes were negative or only lightly positive for CD36. In contrast, in the AME-WD sections, the pattern of hepatocellular positivity for CD36 expanded to encroach upon periportal regions (Figure 3B).

AME-WD elevated hepatic *Cd36* mRNA variants expression

Multiple mRNA variants of *Cd36* have been recorded in Ensembl.org (54), with transcription started from promoter 1, 2, or 3 (Supplemental Figure 1). All the mRNA variants are translated into the same protein product.

Mirroring the expression pattern of *Cd36* total mRNA, both WD and AME had significant effects on the increase of expression of the P2 and P3 transcripts (*P* values < 0.05)

TABLE 3 Measurement of fat, liver, and insulin resistance parameters in day 120 male offspring of Con and AME dams fed postweaning CD or WD

Maternal group	Con		AME		*P* value		
Postweaning diet	CD	WD	CD	WD	Diet	Maternal environment	D × M
Retroperitoneal fat weight, g/100 g BW	0.006 ± 0.001	0.011 ± 0.002[1]	0.007 ± 0.002	0.013 ± 0.002[1]	<0.0001	0.0009	0.815
Liver weight, g/100 g BW	0.036 ± 0.002[2]	0.038 ± 0.002[2]	0.035 ± 0.002[2]	0.049 ± 0.008[3]	0.0003	0.0078	0.0048
Fasting glucose, mmol/L	9.59 ± 1.38	10.2 ± 1.70	10.3 ± 1.01	11.2 ± 1.98	0.198	0.266	0.88
Fasting insulin, ng/mL	3.41 ± 1.80[2]	2.70 ± 1.24[2]	2.89 ± 0.921[2]	7.97 ± 1.89[3]	0.0004	0.0008	<0.0001
HOMA-IR	29.6 ± 14.1[2]	71.5 ± 15.5[2]	33.8 ± 18.3[2]	125 ± 52.6[3]	<0.0001	0.0108	0.0271
AUC glucose in GTT, mol/L·120min	1.65 ± 0.142	2.74 ± 0.483[1]	2.28 ± 0.423	2.70 ± 0.412	0.0005	0.107	0.0676
Insulin 60 min post glucose injection, ng/mL	3.34 ± 0.389	3.82 ± 1.37[1]	3.94 ± 0.891	5.95 ± 1.33[1,4]	0.0025	0.0011	0.051

Data are means ± SDs. $n = 6$. AME, adverse maternal environment; CD, control diet; Con, maternal control group; GTT, glucose tolerance test; WD, western diet.
[1]Different from corresponding postweaning CD group, $P < 0.05$.
[2,3]When the diet × maternal environment interaction was significant, only values with differing superscripts are significant, $P < 0.05$. Values that share a superscript are not significant.
[4]Different from corresponding maternal Con group, $P < 0.05$.

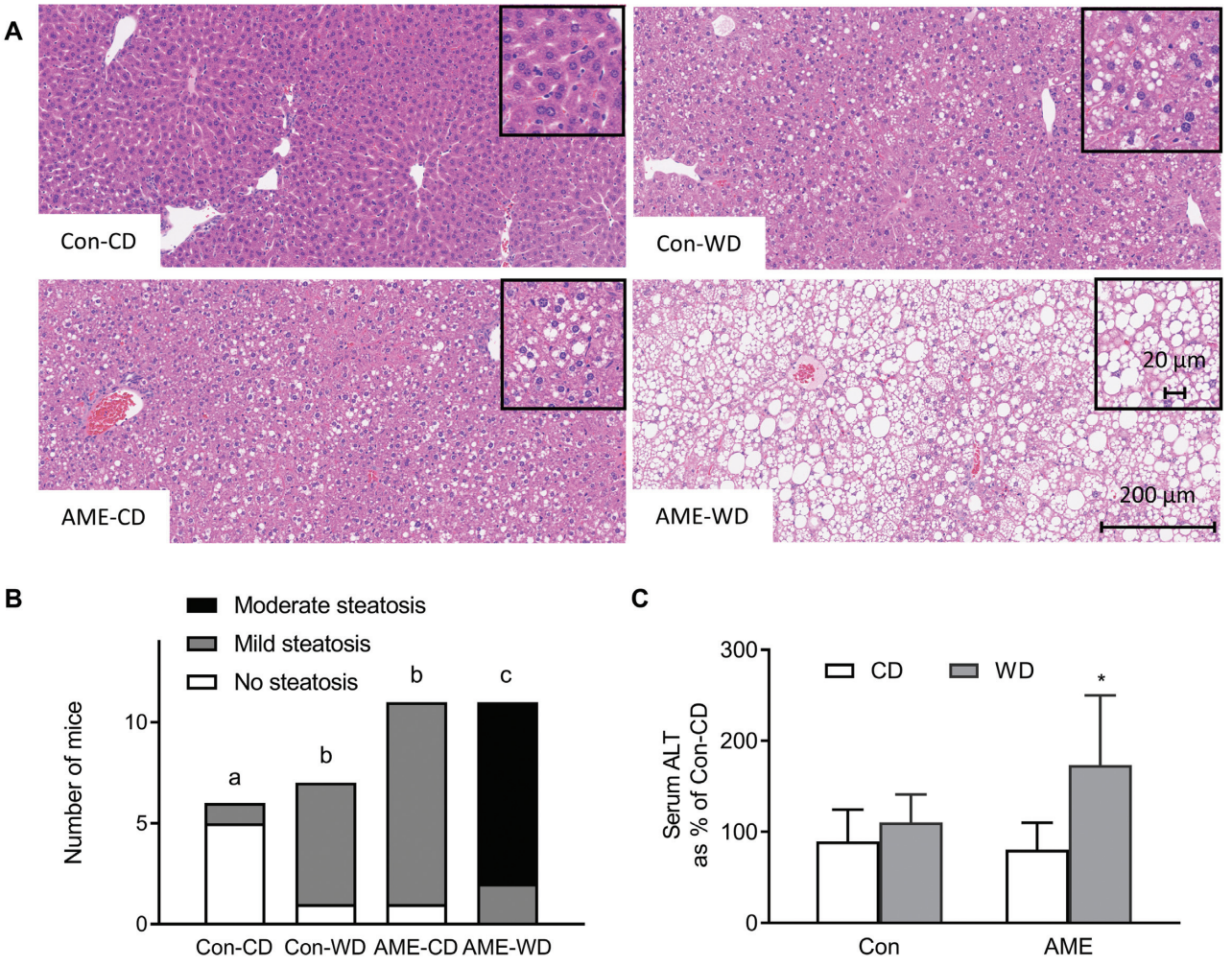

FIGURE 1 Liver histology (A), diagnosis of hepatic steatosis (B), and serum ALT (C) in d120 mice from the Con and AME maternal groups and on the postweaning diet of CD or WD. Representative images were H&E-stained liver sections from each group and are shown as 100× (large images) and 200× (small images) magnifications (A). Values are number of mice diagnosed with varying degrees of hepatic steatosis based on the evaluation results of NAFLD activity scoring. Labeled groups without a common letter differ, $P < 0.05$ (B). Values are means ± SDs. $n = 6$. *Different from corresponding postweaning CD group, $P < 0.05$ (C). ALT, alanine transaminase; AME, adverse maternal environment; CD, control diet; Con, control; H&E, hematoxylin and eosin; WD, Western diet.

(Figure 3C). Furthermore, AME-WD offspring had significantly higher expression of the P2 and P3 transcripts compared with that of Con-WD and AME-CD (P values < 0.05), but no significant interaction between WD and AME was found (P-interactions ≥ 0.05). Promoter 1 transcripts were expressed very low and unaltered by either AME or WD. These findings in mRNA variants indicate that WD and AME activated promoters 2 and 3 to increase transcription initiated from P2 and P3. Together with the altered distribution pattern of CD36$^+$ hepatocytes (Figure 3B) in the AME-WD livers, we speculated that AME-WD had DNA hypomethylation in promoters 2 and 3, but not in promoter 1 region.

AME or WD decreased DNA methylation around *Cd36* promoters 2 and 3

As expected, both WD and AME had significant effects on the DNA hypomethylation across all the studied CpG sites on both promoters 2 and 3 (P values < 0.05) (**Figure 4**A). Importantly, AME-CD was significantly hypomethylated compared with Con-CD in 1 of 2 CpG sites in P2 and 4 of 6 CpG sites in P3 (Figure 4A), indicating AME alone resulted in DNA hypomethylation in *Cd36* promoters 2 and 3 in the offspring. This AME effect on promoter hypomethylation was to a similar extent to that of postweaning WD (P values ≥ 0.05 across all the CpG sites between AME-CD and Con-WD). AME-WD further decreased DNA methylation in 2 of 2 CpG sites of P2 and 4 of 6 CpG sites of P3 compared with the 2 corresponding control groups (Con-WD and AME-CD) (P values < 0.05) (Figure 4A), indicating postweaning WD and AME had additive effects on *Cd36* promoter hypomethylation (P-interaction ≥ 0.05).

These effects of WD and AME on DNA hypomethylation on P2 and P3 of *Cd36* are locus specific because neither WD nor AME had altered CpG methylation in the P1 region (Figure 4A) and the intron 1 region (**Supplemental Figure 2A**).

Promoters 2 and 3 were hypomethylated in CD36$^+$ hepatocytes, vice versa

To verify if the P2 and P3 regions studied were critical for the *Cd36* promoter activity, we quantified DNA methylation of the laser-capture microdissected CD36$^-$ and CD36$^+$ hepatocytes. We expected high methylation in the CD36$^-$ cells but low methylation in the CD36$^+$ cells if the CpG sites are critical to the activity of the corresponding promoters (49, 55).

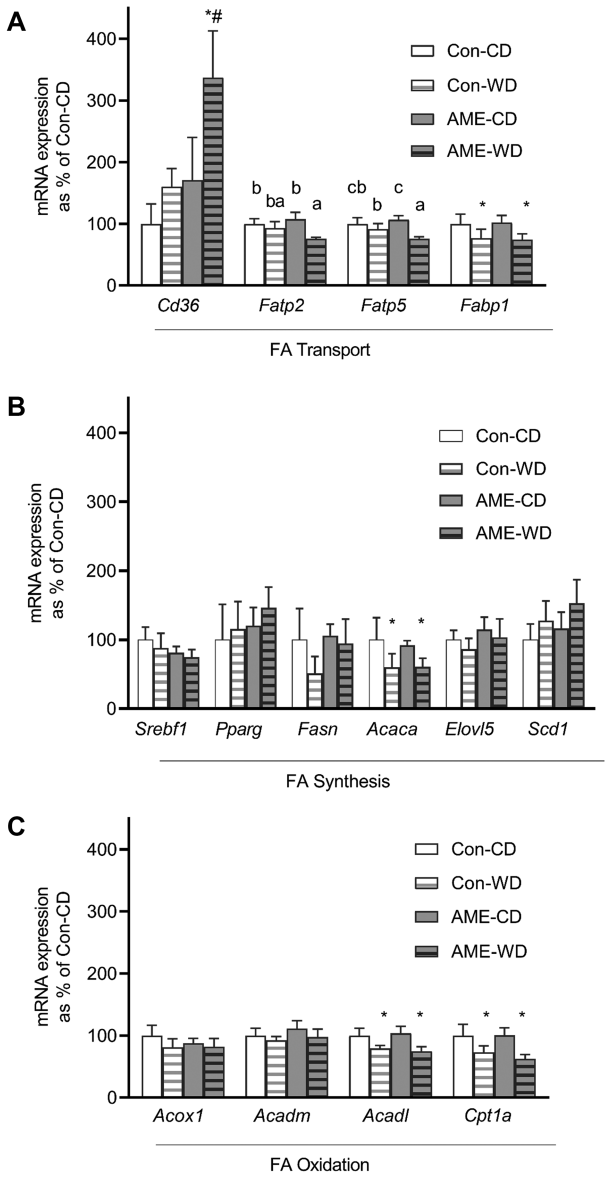

FIGURE 2 Hepatic mRNA expression of genes for FA transport (A), FA synthesis (B), and FA oxidation (C) in d120 mice from the Con and AME maternal groups and on the postweaning diet of CD or WD. Values are means ± SDs. $n = 6$. *Different from corresponding postweaning CD group, $P < 0.05$; #Different from corresponding maternal Con group, $P < 0.05$; When the diet × maternal environment interaction was significant, labeled means without a common letter differ, $P < 0.05$. AME, adverse maternal environment; CD, control diet; Con, control group; FA, fatty acid; WD, western diet.

As expected, CD36$^+$ hepatocytes were significantly hypomethylated compared with CD36$^-$ cells (Figure 4B) in both of the CpG sites in P2 and 2 of the 6 sites in P3 (Figure 4B) (P values < 0.05), indicating that the P2 regions where the studied CpG sites reside and the −804- to −846-bp region of P3 may be critical regulatory regions for the promoter activity of *Cd36* gene. This locus specificity is supported by the lack of significant difference of CpG methylation in promoter 1 (Figure 4B) and intron 1 regions (Supplemental Figure 2B) between CD36$^+$ and CD36$^-$ hepatocytes.

Discussion

The primary finding of this study is that an adverse maternal environment together with postweaning WD results in hepatic steatosis in adult male offspring. In this model the severity of steatosis increases in parallel with elevated hepatic *Cd36* mRNA and protein expression, altered lobular distribution pattern of CD36-expressing hepatocytes, and perturbed intercellular epigenetic heterogeneity of *Cd36* promoter methylation. Additionally, we found that adverse maternal environment alone predisposes the offspring to mild hepatic steatosis concurrent with DNA hypomethylation on the promoters 2 and 3 of *Cd36* and this predisposition is not altered by a low-fat postweaning diet. These findings indicate that adverse maternal environment set the epigenetic background of the offspring's hepatic *Cd36* gene to effectively place the offspring at greater risk for NAFLD when experiencing the ever-common WD later in life.

WD alone has been associated with the increased risk of adult NAFLD in human (56, 57) and animal models (24–30). Additionally, maternal HFD together with HFD in offspring has also been found to result in the onset of NAFLD in offspring (5–9, 31). However, the role of the postweaning diet following maternal stress and diet-induced AME on the development of NAFLD has not been explored. Likewise, the molecular changes associated with AME-induced NAFLD have, to our knowledge, not been explored previously.

Our data demonstrate that an adverse maternal environment coupled with a postweaning WD have an additive effect and cause the development of hepatic steatosis. Importantly, dietary intervention of a low-fat control diet following weaning does not fully correct the development of steatosis. In fact, mice exposed to AME alone develop an extent of steatosis similar to that of mice on a postweaning WD alone. These findings indicate the power and lasting effect of an adverse early life environment.

The relation of *Cd36* mRNA and protein expression and adult hepatic steatosis has been reported in both human and animal studies (19–21, 58). Upregulation of CD36 membrane protein is positively correlated with hepatic steatosis (11, 20, 59) and elevates cellular uptake of fatty acids (11, 59). Inhibition of *Cd36* mRNA (60) and protein ablated the accumulation of lipid in vitro and in vivo (60, 61). Liver-specific *Cd36* knockout attenuates steatosis in mouse models of NAFLD (4, 12). We report that AME alone upregulated hepatic *Cd36* mRNA expression, which is correlated with the presence of mild steatosis. More importantly, this AME-upregulation of *Cd36* mRNA is correlated with the hypomethylation of *Cd36* promoter regions.

The differentially methylated CpG sites in promoters 2 and 3 of *Cd36* found in this study may be important loci for regulating *Cd36* transcription. Both promoters 2 and 3 have been reported to have promoter activities in mice and humans (the *Cd36* gene is conserved between mouse and human) (4, 62, 63). The promoter 2 CpG sites examined here are immediately upstream of the active promoter reported by Sato, et al. (63). The CpG sites we have studied in promoter 3 region are in proximity of the binding sites of well-known steatosis-promoting transcription factors, including liver X receptor, prognane X receptor, and PPARγ (4). Studies have shown that these transcription factors promote hepatic steatosis through *Cd36* activation (4, 64, 65). Importantly, we have revealed 2 regions of environmentally induced epigenetic heterogeneity within *Cd36*. Our findings of environmentally driven DNA hypomethylation of hepatic *Cd36* coupled with increased expression and severity of steatosis are

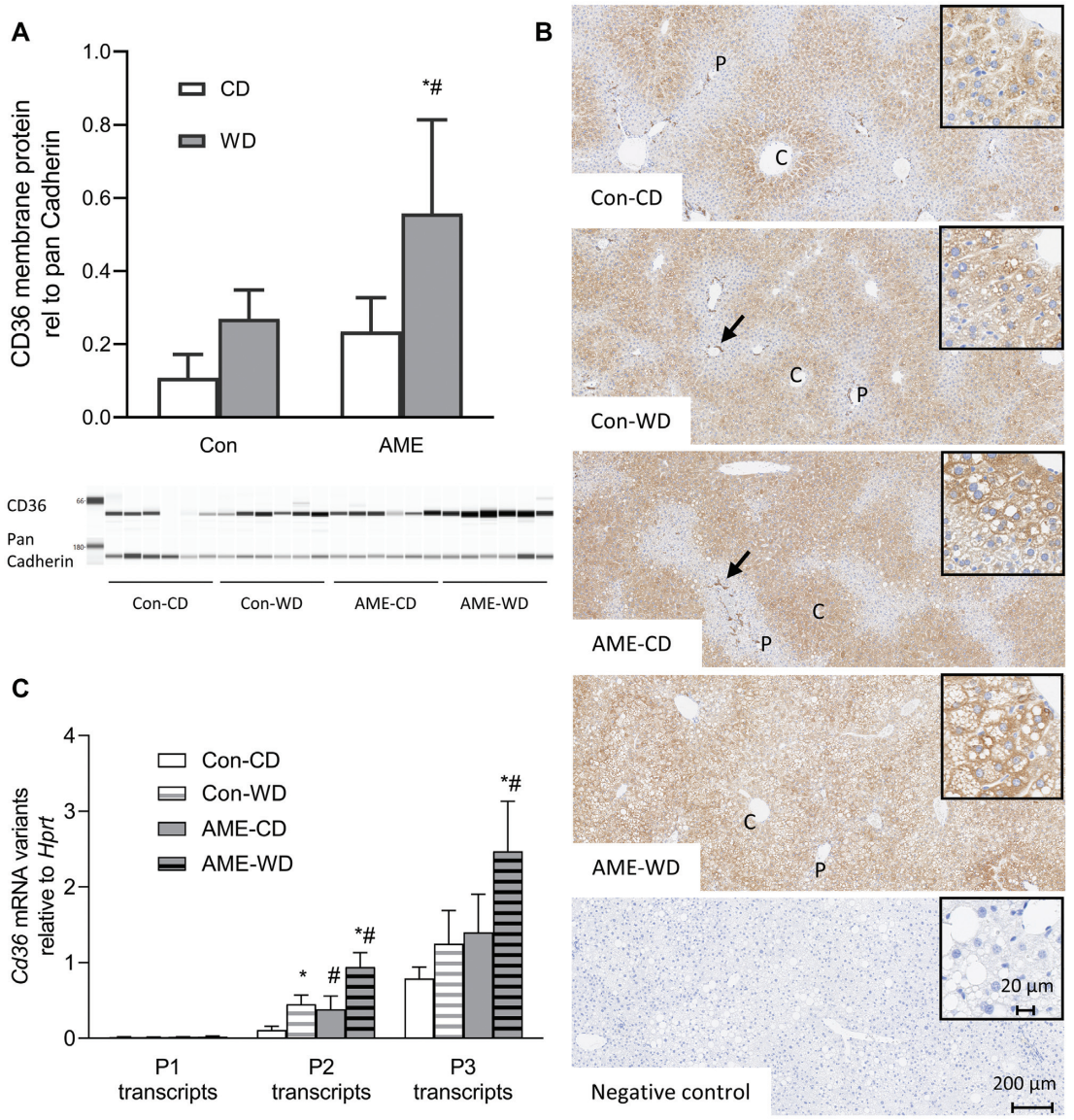

FIGURE 3 CD36 membrane protein expression and immunoblot image (A), CD36 protein immunohistochemistry staining (B), and expression of *Cd36* mRNA variants (C) in the livers of d120 mice from the Con and AME groups and on the postweaning diet of CD or WD. Values are means ± SDs. $n = 6$. *Different from corresponding postweaning CD group, $P < 0.05$; #Different from corresponding maternal Con group, $P < 0.05$; The diet x maternal environment interaction was not significant, $P \geq 0.05$ (A) and (C). Representative images were immunohistochemically stained for CD36 protein and negative control on liver sections from each group and are shown as 50× (large images) and 200× (small images) magnifications (B). Arrows, macrophages strongly expressed CD36. AME, adverse maternal environment; C, the central vein; CD, control diet; Con, control; P, the portal; WD, western diet.

important for the molecular understanding of AME-related NAFLD.

Caution is always necessary when translating the findings of a mouse model to human pathophysiology. We acknowledge that although C57BL/6J mice are useful to study diet-induced obesity and IR, they are not the ideal animal model to investigate the role of inflammation in the development of hepatic steatosis. No single animal model can completely define a human condition considering the diversity of genetics and experience that are intrinsic to humanity.

NAFLD is a pathological state that is attributed to imbalance of multiple factors, including fatty acid influx, fatty acid oxidation, de novo lipogenesis, and triglyceride secretion. This study focuses on the outcome of AME and postweaning WD on CD36 expression and its epigenetic characteristics in offspring. Further studies are needed to understand the pathways by which these environmental conditions mediate changes in *CD36* methylation.

CD36 has complex functions across multiple tissues. This complexity attributes to a broad range of ligands it interacts with. Therefore, protein interactions and post-transcriptional regulation are also very important for further elucidating the role of CD36 in the pathogenesis of NAFLD.

We recognize that further pursuit of mechanisms affecting the relation between promoters 2 and 3 methylation in *Cd36* and hepatic steatosis is necessary. We also recognize that we do not know whether AME in conjunction with WD induced similar molecular and phenotypical changes in female offspring, who do not suffer as severe hepatic steatosis relative to the male

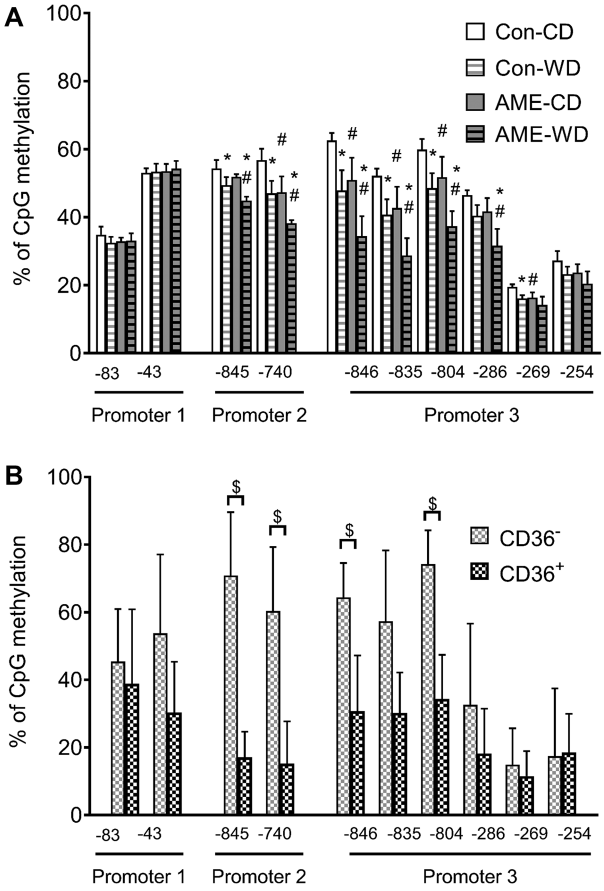

FIGURE 4 DNA CpG methylation of *Cd36* promoters 1, 2, and 3 regions in livers of d120 mouse from the Con and AME maternal groups and on the postweaning diet of CD or WD ($n = 6$) (A) and in laser-capture micro-dissected CD36$^-$ and CD36$^+$ hepatocytes ($n = 3$–4) (B). The negative number below each CpG site indicates the number of base pair upstream relative to the transcription start site of the corresponding exon, respectively. Values are means ± SDs. *Different from corresponding postweaning CD group, $P < 0.05$; #Different from corresponding maternal Con group, $P < 0.05$; The diet x maternal environment interaction was not significant, $P \geq 0.05$; $Different between CD36$^-$ and CD36$^+$ hepatocytes, $P < 0.05$. AME, adverse maternal environment; CD, control diet; Con, control group; WD, western diet.

counterparts. Further studies would be necessary to elucidate sex differences in the future.

NAFLD is a common disease with a growing worldwide prevalence and burden. Understanding how environmental factors like adverse maternal environments contribute to the disease is of increasing importance. Additionally, identifying molecular targets, such as changes in *Cd36* expression and methylation, is critical in the path to ameliorate disease burden.

Acknowledgments

The authors' responsibilities were as follows—AVM, RHL, and QF: designed research; QF, AVM, XK, KAF, and YWH: conducted research; PEN: evaluated NAFLD activity score; QF and AVM: analyzed and interpreted data; QF and AVM: drafted the article; AVM and RHL: critically revised the article; and all authors read and approved the final manuscript.

References

1. Browning JD, Szczepaniak LS, Dobbins R, Nuremberg P, Horton JD, Cohen JC, Grundy SM, Hobbs HH. Prevalence of hepatic steatosis in an urban population in the United States: impact of ethnicity. Hepatology 2004;40(6):1387–95.
2. Angulo P. Nonalcoholic fatty liver disease. N Engl J Med 2002;346(16):1221–31.
3. Cohen JC, Horton JD, Hobbs HH. Human fatty liver disease: old questions and new insights. Science 2011;332(6037):1519–23.
4. Zhou J, Febbraio M, Wada T, Zhai Y, Kuruba R, He J, Lee JH, Khadem S, Ren S, Li S, et al. Hepatic fatty acid transporter Cd36 is a common target of LXR, PXR, and PPARgamma in promoting steatosis. Gastroenterology 2008;134(2):556–67.e1.
5. Wankhade UD, Zhong Y, Kang P, Alfaro M, Chintapalli SV, Piccolo BD, Mercer KE, Andres A, Thakali KM, Shankar K. Maternal high-fat diet programs offspring liver steatosis in a sexually dimorphic manner in association with changes in gut microbial ecology in mice. Sci Rep 2018;8(1):16502.
6. Mouralidarane A, Soeda J, Sugden D, Bocianowska A, Carter R, Ray S, Saraswati R, Cordero P, Novelli M, Fusai G, et al. Maternal obesity programs offspring non-alcoholic fatty liver disease through disruption of 24-h rhythms in mice. Int J Obes 2015;39(9):1339–48.
7. Bruce KD, Cagampang FR, Argenton M, Zhang J, Ethirajan PL, Burdge GC, Bateman AC, Clough GF, Poston L, Hanson MA, et al. Maternal high-fat feeding primes steatohepatitis in adult mice offspring, involving mitochondrial dysfunction and altered lipogenesis gene expression. Hepatology 2009;50(6):1796–808.
8. Tiao MM, Lin YJ, Yu HR, Sheen JM, Lin IC, Lai YJ, Tain YL, Huang LT, Tsai CC. Resveratrol ameliorates maternal and post-weaning high-fat diet-induced nonalcoholic fatty liver disease via renin-angiotensin system. Lipids Health Disease 2018;17(1):178.
9. McCurdy CE, Bishop JM, Williams SM, Grayson BE, Smith MS, Friedman JE, Grove KL. Maternal high-fat diet triggers lipotoxicity in the fetal livers of nonhuman primates. J Clin Invest 2009;119(2):323–35.
10. Bradbury MW. Lipid metabolism and liver inflammation. I. Hepatic fatty acid uptake: possible role in steatosis. Am J Physiol Gastrointest Liver Physiol 2006;290(2):G194–8.
11. Koonen DP, Jacobs RL, Febbraio M, Young ME, Soltys CL, Ong H, Vance DE, Dyck JR. Increased hepatic CD36 expression contributes to dyslipidemia associated with diet-induced obesity. Diabetes 2007;56(12):2863–71.
12. Wilson CG, Tran JL, Erion DM, Vera NB, Febbraio M, Weiss EJ. Hepatocyte-specific disruption of CD36 attenuates fatty liver and improves insulin sensitivity in HFD-fed mice. Endocrinology 2016;157(2):570–85.
13. Rada P, Gonzalez-Rodriguez A, Garcia-Monzon C, Valverde AM. Understanding lipotoxicity in NAFLD pathogenesis: is CD36 a key driver? Cell Death Dis 2020;11(9):802.
14. Ehehalt R, Fullekrug J, Pohl J, Ring A, Herrmann T, Stremmel W. Translocation of long chain fatty acids across the plasma membrane–lipid rafts and fatty acid transport proteins. Mol Cell Biochem 2006;284(1-2):135–40.
15. Su X, Abumrad NA. Cellular fatty acid uptake: a pathway under construction. Trends Endocrinol Metabol 2009;20(2):72–77.
16. Samovski D, Sun J, Pietka T, Gross RW, Eckel RH, Su X, Stahl PD, Abumrad NA. Regulation of AMPK activation by CD36 links fatty acid uptake to beta-oxidation. Diabetes 2015;64(2):353–9.
17. Nassir F, Adewole OL, Brunt EM, Abumrad NA. CD36 deletion reduces VLDL secretion, modulates liver prostaglandins, and exacerbates hepatic steatosis in ob/ob mice. J Lipid Res 2013;54(11):2988–97.
18. Li Y, Yang P, Zhao L, Chen Y, Zhang X, Zeng S, Wei L, Varghese Z, Moorhead JF, Chen Y, et al. CD36 plays a negative role in the regulation of lipophagy in hepatocytes through an AMPK-dependent pathway. J Lipid Res 2019;60(4):844–55.
19. Bechmann LP, Gieseler RK, Sowa JP, Kahraman A, Erhard J, Wedemeyer I, Emons B, Jochum C, Feldkamp T, Gerken G, et al. Apoptosis is associated with CD36/fatty acid translocase upregulation in non-alcoholic steatohepatitis. Liver Int 2010;30(6):850–9.
20. Miquilena-Colina ME, Lima-Cabello E, Sanchez-Campos S, Garcia-Mediavilla MV, Fernandez-Bermejo M, Lozano-Rodriguez T, Vargas-Castrillon J, Buque X, Ochoa B, Aspichueta P, et al. Hepatic fatty acid translocase CD36 upregulation is associated with insulin

resistance, hyperinsulinaemia and increased steatosis in non-alcoholic steatohepatitis and chronic hepatitis C. Gut 2011;60(10):1394–402.
21. Greco D, Kotronen A, Westerbacka J, Puig O, Arkkila P, Kiviluoto T, Laitinen S, Kolak M, Fisher RM, Hamsten A, et al. Gene expression in human NAFLD. Am J Physiol Gastrointest Liver Physiol 2008;294(5):G1281–7.
22. Zhao L, Zhang C, Luo X, Wang P, Zhou W, Zhong S, Xie Y, Jiang Y, Yang P, Tang R, et al. CD36 palmitoylation disrupts free fatty acid metabolism and promotes tissue inflammation in non-alcoholic steatohepatitis. J Hepatol 2018;69(3):705–17.
23. Sheedfar F, Sung MM, Aparicio-Vergara M, Kloosterhuis NJ, Miquilena-Colina ME, Vargas-Castrillon J, Febbraio M, Jacobs RL, de Bruin A, Vinciguerra M, et al. Increased hepatic CD36 expression with age is associated with enhanced susceptibility to nonalcoholic fatty liver disease. Aging 2014;6(4):281–95.
24. Lim JS, Mietus-Snyder M, Valente A, Schwarz JM, Lustig RH. The role of fructose in the pathogenesis of NAFLD and the metabolic syndrome. Nat Rev Gastroenterol Hepatol 2010;7(5):251–64.
25. Jiang JX, Chen X, Fukada H, Serizawa N, Devaraj S, Torok NJ. Advanced glycation endproducts induce fibrogenic activity in nonalcoholic steatohepatitis by modulating TNF-alpha-converting enzyme activity in mice. Hepatology 2013;58(4):1339–48.
26. Gariani K, Ryu D, Menzies KJ, Yi HS, Stein S, Zhang H, Perino A, Lemos V, Katsyuba E, Jha P, et al. Inhibiting poly ADP-ribosylation increases fatty acid oxidation and protects against fatty liver disease. J Hepatol 2017;66(1):132–41.
27. Dorn C, Engelmann JC, Saugspier M, Koch A, Hartmann A, Muller M, Spang R, Bosserhoff A, Hellerbrand C. Increased expression of c-Jun in nonalcoholic fatty liver disease. Lab Invest 2014;94(4):394–408.
28. Grande F, Anderson JT, Keys A. Sucrose and various carbohydrate-containing foods and serum lipids in man. Am J Clin Nutr 1974;27(10):1043–51.
29. Schattenberg JM, Galle PR. Animal models of non-alcoholic steatohepatitis: of mice and man. Dig Dis 2010;28(1):247–54.
30. Wang D, Wei Y, Pagliassotti MJ. Saturated fatty acids promote endoplasmic reticulum stress and liver injury in rats with hepatic steatosis. Endocrinology 2006;147(2):943–51.
31. Zhou L, Liu D, Wang Z, Dong H, Xu X, Zhou S. Establishment and comparison of juvenile female mouse models of nonalcoholic fatty liver disease and nonalcoholic steatohepatitis. Gastroenterol Res Pract 2018;2018:1.
32. Lee HS. Impact of maternal diet on the epigenome during in utero life and the developmental programming of diseases in childhood and adulthood. Nutrients 2015;7(11):9492–507.
33. Waterland RA, Jirtle RL. Transposable elements: targets for early nutritional effects on epigenetic gene regulation. Mol Cell Biol 2003;23(15):5293–300.
34. Ke X, Fu Q, Sterrett J, Hillard CJ, Lane RH, Majnik A. Adverse maternal environment and western diet impairs cognitive function and alters hippocampal glucocorticoid receptor promoter methylation in male mice. Physiol Rep 2020;8(8):e14407.
35. Depner CM, Philbrick KA, Jump DB. Docosahexaenoic acid attenuates hepatic inflammation, oxidative stress, and fibrosis without decreasing hepatosteatosis in a Ldlr(-/-) mouse model of western diet-induced nonalcoholic steatohepatitis. J Nutr 2013;143(3):315–23.
36. Antunes LC, Elkfury JL, Jornada MN, Foletto KC, Bertoluci MC. Validation of HOMA-IR in a model of insulin-resistance induced by a high-fat diet in Wistar rats. Arch Endocrinol Metabol 2016;60(2):138–42.
37. Cacho J, Sevillano J, de Castro J, Herrera E, Ramos MP. Validation of simple indexes to assess insulin sensitivity during pregnancy in Wistar and Sprague-Dawley rats. Am J Physiol Endocrinol Metabol 2008;295(5):E1269–76.
38. Lee S, Muniyappa R, Yan X, Chen H, Yue LQ, Hong EG, Kim JK, Quon MJ. Comparison between surrogate indexes of insulin sensitivity and resistance and hyperinsulinemic euglycemic clamp estimates in mice. Am J Physiol Endocrinol Metabol 2008;294(2):E261–70.
39. Petito-da-Silva TI, Souza-Mello V, Barbosa-da-Silva S. Empaglifozin mitigates NAFLD in high-fat-fed mice by alleviating insulin resistance, lipogenesis and ER stress. Mol Cell Endocrinol 2019;498:110539.
40. Mayurasakorn K, Hasanah N, Homma T, Homma M, Rangel IK, Garza AE, Romero JR, Adler GK, Williams GH, Pojoga LH. Caloric restriction improves glucose homeostasis, yet increases cardiometabolic risk in caveolin-1-deficient mice. Metabolism 2018;83:92–101.
41. Adkins Y, Schie IW, Fedor D, Reddy A, Nguyen S, Zhou P, Kelley DS, Wu J. A novel mouse model of nonalcoholic steatohepatitis with significant insulin resistance. Lab Invest 2013;93(12):1313–22.
42. Ji Y, Gao Y, Chen H, Yin Y, Zhang W. Indole-3-acetic acid alleviates nonalcoholic fatty liver disease in mice via attenuation of hepatic lipogenesis, and oxidative and inflammatory stress. Nutrients 2019;11(9):2062.
43. Matthews DR, Hosker JP, Rudenski AS, Naylor BA, Treacher DF, Turner RC. Homeostasis model assessment: insulin resistance and beta-cell function from fasting plasma glucose and insulin concentrations in man. Diabetologia 1985;28(7):412–9.
44. McGuinness OP, Ayala JE, Laughlin MR, Wasserman DH. NIH experiment in centralized mouse phenotyping: the Vanderbilt experience and recommendations for evaluating glucose homeostasis in the mouse. Am J Physiol Endocrinol Metabol 2009;297(4):E849–55.
45. Ayala JE, Samuel VT, Morton GJ, Obici S, Croniger CM, Shulman GI, Wasserman DH, McGuinness OP, Consortium NIHMMPC. Standard operating procedures for describing and performing metabolic tests of glucose homeostasis in mice. Dis Model Mech 2010;3(9–10):525–34.
46. Kleiner DE, Brunt EM, Van Natta M, Behling C, Contos MJ, Cummings OW, Ferrell LD, Liu YC, Torbenson MS, Unalp-Arida A, et al. Design and validation of a histological scoring system for nonalcoholic fatty liver disease. Hepatology 2005;41(6):1313–21.
47. Fu Q, Yu X, Callaway CW, Lane RH, McKnight RA. Epigenetics: intrauterine growth retardation (IUGR) modifies the histone code along the rat hepatic IGF-1 gene. FASEB J 2009;23(8):2438–49.
48. Kunjathoor VV, Febbraio M, Podrez EA, Moore KJ, Andersson L, Koehn S, Rhee JS, Silverstein R, Hoff HF, Freeman MW. Scavenger receptors class A-I/II and CD36 are the principal receptors responsible for the uptake of modified low density lipoprotein leading to lipid loading in macrophages. J Biol Chem 2002;277(51):49982–8.
49. Stadler MB, Murr R, Burger L, Ivanek R, Lienert F, Scholer A, van Nimwegen E, Wirbelauer C, Oakeley EJ, Gaidatzis D, et al. DNA-binding factors shape the mouse methylome at distal regulatory regions. Nature 2011;480(7378):490–5.
50. Shen L, Guo Y, Chen X, Ahmed S, Issa JP. Optimizing annealing temperature overcomes bias in bisulfite PCR methylation analysis. BioTechniques 2007;42(1):48, 50, 2 passim.
51. Seltman HJ. Experimental design and analysis. Carnegie Mellow University; 2012 [Cited 2021 Aug 8]. http://www.stat.cmu.edu/~hseltman/309/Book/.
52. Benjamini Y, Krieger AM, Yekutieli D. Adaptive linear step-up procedures that control the false discovery rate. Biometrika 2006;93(3):491–507.
53. Roell KR, Reif DM, Motsinger-Reif AA. An Introduction to terminology and methodology of chemical synergy-perspectives from across disciplines. Front Pharmacol 2017;8:158.
54. Howe KL, Contreras-Moreira B, De Silva N, Maslen G, Akanni W, Allen J, Alvarez-Jarreta J, Barba M, Bolser DM, Cambell L, et al. Ensembl Genomes 2020-enabling non-vertebrate genomic research. Nucleic Acids Res 2020;48(D1):D689–95.
55. Feldmann A, Ivanek R, Murr R, Gaidatzis D, Burger L, Schubeler D. Transcription factor occupancy can mediate active turnover of DNA methylation at regulatory regions. PLos Genet 2013;9(12):e1003994.
56. Zelber-Sagi S, Nitzan-Kaluski D, Goldsmith R, Webb M, Blendis L, Halpern Z, Oren R. Long term nutritional intake and the risk for non-alcoholic fatty liver disease (NAFLD): a population based study. J Hepatol 2007;47(5):711–7.
57. Oddy WH, Herbison CE, Jacoby P, Ambrosini GL, O'Sullivan TA, Ayonrinde OT, Olynyk JK, Black LJ, Beilin LJ, Mori TA, et al. The Western dietary pattern is prospectively associated with nonalcoholic fatty liver disease in adolescence. Am J Gastroenterol 2013;108(5):778–85.
58. Buque X, Martinez MJ, Cano A, Miquilena-Colina ME, Garcia-Monzon C, Aspichueta P, Ochoa B. A subset of dysregulated metabolic and survival genes is associated with severity of hepatic steatosis in obese Zucker rats. J Lipid Res 2010;51(3):500–13.
59. Luiken JJ, Arumugam Y, Dyck DJ, Bell RC, Pelsers MM, Turcotte LP, Tandon NN, Glatz JF, Bonen A. Increased rates of fatty acid uptake and plasmalemmal fatty acid transporters in obese Zucker rats. J Biol Chem 2001;276(44):40567–73.

60. Lin HY, Wang FS, Yang YL, Huang YH. MicroRNA-29a suppresses CD36 to ameliorate high fat diet-induced steatohepatitis and liver fibrosis in mice. Cells 2019;8(10):1298.
61. Lebeau PF, Byun JH, Platko K, Al-Hashimi AA, Lhotak S, MacDonald ME, Mejia-Benitez A, Prat A, Igdoura SA, Trigatti B, et al. Pcsk9 knockout exacerbates diet-induced non-alcoholic steatohepatitis, fibrosis and liver injury in mice. JHEP Reports 2019;1(6):418–29.
62. Barclay JL, Nelson CN, Ishikawa M, Murray LA, Kerr LM, McPhee TR, Powell EE, Waters MJ. GH-dependent STAT5 signaling plays an important role in hepatic lipid metabolism. Endocrinology 2011;152(1):181–92.
63. Sato O, Kuriki C, Fukui Y, Motojima K. Dual promoter structure of mouse and human fatty acid translocase/CD36 genes and unique transcriptional activation by peroxisome proliferator-activated receptor alpha and gamma ligands. J Biol Chem 2002;277(18):15703–11.
64. Zhou J, Zhai Y, Mu Y, Gong H, Uppal H, Toma D, Ren S, Evans RM, Xie W. A novel pregnane X receptor-mediated and sterol regulatory element-binding protein-independent lipogenic pathway. J Biol Chem 2006;281(21):15013–20.
65. Zhang C, Luo X, Chen J, Zhou B, Yang M, Liu R, Liu D, Gu HF, Zhu Z, Zheng H, et al. Osteoprotegerin promotes liver steatosis by targeting the ERK-PPAR-gamma-CD36 pathway. Diabetes 2019;68(10):1902–14.